Hierarchic Plate and Shell Theories with Direct Evaluation of Transverse Electric Displacement

E. Carrera*, P. Nali†, S. Brischetto‡, M. Cinefra§

Aerospace Department (DIASP), Politecnico di Torino, Corso Duca degli Abruzzi, 24, 10129, Torino, Italy

A mixed variational statement for the analysis of layered structures under the effect of mechanical and electrical fields is proposed in this paper to develop finite plate elements what permits direct evaluation (that is "a priori") of transverse electrical displacement D_z. The original Reissner Mixed Variational Theorem RMVT is modified to account "only" for interlaminar continuous D_z. Continuity of mechanical variables, such as transverse shear and normal stress components, is discarded to provide a simple "Electrical" modified RMVT, here denoted RMVT-D_z. Implementation are made via Carrera Unified Formulation. The applications of the proposed approach is demonstrated by comparison with classical formulations based on the Principle of Virtual Displacements as well as to available 3D and analytical solutions.

I. Introduction

Smart systems can be considered the candidates for next generation structures in aerospace vehicles as well as for some advanced products in the automotive and ship industries. Piezoelectric materials are extensively used in this framework. These materials are characterized by the so-called "direct" and "inverse effect": an applied electrical potential induces mechanical stresses and vice-versa. Such an electro-mechanical coupling permits one to build closed-loop control systems in which piezo-materials play the role of both actuators and sensors. An intelligent structure can therefore be built in which, for instance, deformations or vibrations are reduced by appropriate control laws.

An appropriate use of piezoelectric materials, however requires an accurate description of the electrical and mechanical fields in the constitutive layers. The present paper focuses on the computational, finite element, electro-mechanical two-dimensional modelings of smart structures embedding piezo layers.

Piezoelectric plates appear as multilayered structures. Very often, piezoelectric layers are embedded in laminated structures made of anisotropic composite materials. The importance of appropriate modelings of piezoelectric plates is clearly displayed by the large number of papers that have been published over the last two decades.

Among the available review papers, those by Saravanos and Heyliger,[1] and Wang and Yan[2] are herein mentioned. A short review of some of the latest contributions to the FE analysis of piezoelectric plates follows. A finite element that includes a FSDT description of displacements and layer-wise form of the electric potential was developed by Sheik et al.[3] The numerical, membrane and bending behavior of FEs which are based on FSDT was analyzed by Auricchio et al.[4] in the framework of a suitable variational formulation. The third order theory of HOT type was applied by Thornburg and Chattopadhyay[5] to derive finite elements that take into consideration the electro-mechanical coupling. Similar elements have more recently been considered by Shu.[6] The extension of the third order Zig-Zag Ambartsumian multilayered theory to finite analysis of electromechanical problems has been proposed by Oh and Cho.[7] An extension to piezoelectricity of numerically efficient plate/shell elements based on the Mixed Interpolation of Tensorial Components (MITC) formulation has recently been provided by Kögl and Bucalem.[8,9]

Although traditional layer-wise theories, based on the Principle of Virtual Displacements (PVD), are able

*Professor, Politecnico di Torino, erasmo.carrera@polito.it.
†PhD Student, Politecnico di Torino, pietro.nali@polito.it.
‡PhD, Politecnico di Torino, salvatore.brischetto@polito.it.
§PhD Student, Politecnico di Torino, maria.cinefra@polito.it.

to accurately predict mechanical displacements, electric potential, in-plane stress and in-plane electric displacements, they are unable to guarantee the continuity of transverse stresses or of the transverse electric displacement at the interface between two adjacent layers (the continuity of transverse stresses should be enforced for equilibrium reasons). The continuity conditions for secondary variables, such as transverse stresses and transverse electric displacement, are known in literature as C_z^0 requirements.[10] These requirements can be satisfied by employing the mixed approach. In particular, displacement components, electric potential, transverse stresses and transverse electric displacement can be independently considered and used as degrees of freedom, using the Reissner Mixed Variational Theorem (RMVT).[11,12] In this way, the continuity of transverse stresses and of the transverse electric displacement is always guaranteed and, consequently, the C_z^0 requirements are automatically fulfilled. On most of the last decade, the first author and his co-workers have contributed extensively to the application of RMVT to multilayered made structures and they have introduced a layer-wise finite element formulation for composite plates that fulfils the continuity of transverse stresses between layers.[13] Closed-form solution analysis as well as FE applications[14] have shown that RMVT can be considered a very suitable tool to provide a quasi-3D description of stress and strain fields in anisotropic laminated structures. The formulation employed in these latter works, named Carrera Unified Formulation (CUF), permits one to formulate both ESL and LW models in terms of a few "Fundamental Nuclei" whose form does not depend on either the order of the through-the-thickness expansion that has been used for the various variables or on the number of nodes of the element. Many works have been devoted to the extension of the CUF: PVD and RMVT variational statements where extended to piezolaminated plates.[15] The modeling of piezolaminated plates using layerwise mixed finite elements was then proposed[16] and subsequently an extension of the RMVT to piezoelectric laminates with analytical results was published.[17] Mixed finite elements for static and dynamics analysis of piezoelectric plates have been provided,[18] where only transverse stresses were modeled by RMVT. The related variational statement has been named P-RMVT, where the "P" stands for "Partial". In this case, the transverse electric displacement D_z was calculated by post-processing. More accurate results for the evaluation of the D_z have been presented in a recent work,[19] where the transverse stresses, together with the D_z, have been modeled by RMVT. The employed variational statement has been called F-RMVT, where the "F" stands for "Full".
Among the various variables, the evaluation of the transverse electric displacement is of particular interest. The D_z is, in fact, closely related to the electrical charge Q:

$$Q = \int_\Omega D_z \, d\Omega, \tag{1}$$

where Ω is the plate surface. The charge consists of a fundamental input/output in a closed-loop control of a smart structure. Faster and accurate evaluation of Q is a key-point in the development of an efficient and reliable closed-loop control algorithm. However, D_z, in classical applications is only given "a posteriori" via post-processing of the primary variables (the displacements and the electrical potential). An extended RMVT application, with D_z assumed as primary variable, has been employed in this paper, which has been called RMVT-D_z. The relevant difference between RMVT-D_z and the above mentioned F-RMVT is that the first does not imply the modeling of transverse stresses, while both variational statements require the modeling of the transverse electric displacement. As a consequence, RMVT-D_z leads to a lower computational effort than F-RMVT and it assures, at the same time, accurate results for the transverse electric displacement. An almost complete overview of the possible subcases of RMVT was given in a recent paper.[20] The RMVT-D_z was in the latter article mentioned as a possible extension of RMVT to piezoelectric structures. However, constitutive equations and FE matrices consistent with RMVT-D_z were not listed. The present work derives the constitutive equations for RMVT-D_z and develop applications for plate elements in the framework of the CUF. The RMVT-D_z Fundamental Nucleus (explicitly given in the Appendix) contains information to built the corresponding stiffness matrix and in this paper is presented and numerically assessed.

II. Considered variational statements

A. The PVD for the electro-mechanical case

The PVD statement for the pure-mechanical case study is commonly written as it follows:

$$\int_V (\delta \boldsymbol{\epsilon}_G^T \, \boldsymbol{\sigma}_H) \, dV \; = \; \delta L_e, \tag{2}$$

where superscript "T" indicates the array transposition, δ is the variational symbol and bold letters denote arrays. Subscripts "G" and "H" indicates variables obtained by Geometrical relations and by constitutive/Hooke's relations respectively. σ, ϵ and L_e indicate stresses, strains and the external work, in the same sequence.
In the case of applied electro-mechanical loading on a surface Ω, employing Einstein's summation convention over repeated indices, the virtual variation of the external work can be expressed as:

$$\delta L_e = \int_\Omega \left(\bar{t}_i \, \delta u_i - \bar{Q} \, \delta \phi \right) \, d\Omega, \tag{3}$$

where:
$\bar{t}_i$ is the mechanical loading in i-direction (pressure);
u_i is the displacement component in i-direction;
$\bar{Q}$ is the charge density on the plate surface;
ϕ is the electric potential.
Stresses and strains are conveniently split between in-plane and out-of-plane (normal or transverse) components:[20]

$$\int_V (\delta \boldsymbol{\epsilon}_{pG}^T \, \boldsymbol{\sigma}_{pH} + \delta \boldsymbol{\epsilon}_{nG}^T \, \boldsymbol{\sigma}_{nH}) \, dV \; = \; \delta L_e, \tag{4}$$

with:
$\boldsymbol{\epsilon}_p^T = \left\{ \begin{array}{ccc} \epsilon_{xx} & \epsilon_{yy} & \epsilon_{xy} \end{array} \right\}$; $\boldsymbol{\sigma}_p^T = \left\{ \begin{array}{ccc} \sigma_{xx} & \sigma_{yy} & \sigma_{xy} \end{array} \right\}$;
$\boldsymbol{\epsilon}_n^T = \left\{ \begin{array}{ccc} \epsilon_{zz} & \epsilon_{xz} & \epsilon_{yz} \end{array} \right\}$; $\boldsymbol{\sigma}_n^T = \left\{ \begin{array}{ccc} \sigma_{zz} & \sigma_{xz} & \sigma_{yz} \end{array} \right\}$.
Cartesian x, y, z reference system is considered and notation already used in previous work[19] is referred to: subscript "p" denotes in-plane unknowns and subscript "n" denotes out-of-plane unknowns; subscript "z" indicates the through-the-thickness z-direction, while subscripts "x" and "y" are for the two in-plane directions.
If electrical contributions are included, the PVD in Eq.(4) becomes:

$$\int_V (\delta \boldsymbol{\epsilon}_{pG}^T \, \boldsymbol{\sigma}_{pH} + \delta \boldsymbol{\epsilon}_{nG}^T \, \boldsymbol{\sigma}_{nH} \delta - \delta \boldsymbol{E}_{pG}^T \, \boldsymbol{D}_{pH} - \delta E_{nG} \, D_{nH}) \, dV \; = \; \delta L_e, \tag{5}$$

with:
$\boldsymbol{E}_p^T = \left\{ \begin{array}{cc} E_x & E_y \end{array} \right\}$; $\boldsymbol{D}_p^T = \left\{ \begin{array}{cc} D_x & D_y \end{array} \right\}$;
$E_n = \left\{ \begin{array}{c} E_z \end{array} \right\}$; $D_n = \left\{ \begin{array}{c} D_z \end{array} \right\}$.
D and E indicate the transverse electric displacement and the electric field, respectively.
The condensed vectorial notation already discussed[20] is employed in present work. The two multifield variables are introduced:

$$\boldsymbol{\mathcal{S}}^T = \left\{ \begin{array}{cccccccc} \sigma_{xx} & \sigma_{yy} & \sigma_{xy} & -D_x & -D_y & \sigma_{zz} & \sigma_{xz} & \sigma_{yz} & -D_z \end{array} \right\}, \tag{6}$$

$$\boldsymbol{\mathcal{E}}^T = \left\{ \begin{array}{cccccccc} \epsilon_{xx} & \epsilon_{yy} & \epsilon_{xy} & E_x & E_y & \epsilon_{zz} & \epsilon_{xz} & \epsilon_{yz} & E_z \end{array} \right\}, \tag{7}$$

where $\boldsymbol{\mathcal{S}}$ is the vector of extensive variables and $\boldsymbol{\mathcal{E}}$ is the vector of intensive ones. D_z and D_n are the same quantity expressed in different notation.
It is possible to rewrite Eq.(5) in form as simple as Eq.(2) for multifield problems:

$$\int_V \left(\delta \boldsymbol{\mathcal{E}}_G^T \, \boldsymbol{\mathcal{S}}_H \right) dV \; = \; \delta L_e. \tag{8}$$

B. The RMVT-D_z

The advantage of using RMVT consists in the possibility of assuming two independent set of variables: a set of primary unknowns and a set of extensive variables which are modeled in the thickness plate z-direction. This leads to the "a-priori" and complete fulfillment of the interlaminar continuity for the modeled extensive variables, with consequent satisfaction of the C_z^0 requirements in.[13] As stated in the introduction, the

RMVT has been commonly employed to obtain accurate results for transverse stresses in pure mechanical problems.[11] In piezoelectric applications, RMVT has been recently extended to model the transverse electric displacement other than normal stresses.[18]
This work represents the first application of the RMVT with only the electric displacement D_z modeled in the thickness plate z-direction. The convenience of that is explained in the introduction.
The RMVT statement with "a-priori" modeling of the transverse electric displacement D_z (or D_n) is here called RMVT-D_z and it appears in literature according to the following form:[20]

$$\int_V (\delta\boldsymbol{\epsilon}_{pG}^T\,\boldsymbol{\sigma}_{pH} + \delta\boldsymbol{\epsilon}_{nG}^T\,\boldsymbol{\sigma}_{nH} - \delta\boldsymbol{E}_{pG}^T\,\boldsymbol{D}_{pH} - \delta E_{nG}\,D_n - \delta D_n(E_{nG} - E_{nH}))\,dV \;=\; \delta L_e. \tag{9}$$

By referring to the condensed notation and considering that subscript "a" indicates " not modeled quantities", while subscripts "b" are related to "modeled quantities", the following vectors can be introduced:
$\boldsymbol{\mathcal{S}}_{aH} = \left\{ \begin{array}{cccccccc} \sigma_{xx} & \sigma_{yy} & \sigma_{xy} & -D_x & -D_y & \sigma_{zz} & \sigma_{xz} & \sigma_{yz} \end{array} \right\}_H$ is the vector of not-modeled extensive variables, which are calculated by constitutive relations;
$\boldsymbol{\mathcal{S}}_b = \left\{ \begin{array}{c} -D_z \end{array} \right\}$ is the vector of modeled extensive variables;
$\boldsymbol{\mathcal{E}}_{aG} = \left\{ \begin{array}{cccccccc} \epsilon_{xx} & \epsilon_{yy} & \epsilon_{xy} & E_1 & E_2 & \epsilon_{zz} & \epsilon_{xz} & \epsilon_{yz} \end{array} \right\}_G$ is the vector of intensive variables associated to $\boldsymbol{\mathcal{S}}_a$ and calculated by geometrical relations;
$\boldsymbol{\mathcal{E}}_{bG} = \left\{ \begin{array}{c} E_z \end{array} \right\}_G$ is the vector of intensive variables associated to $\boldsymbol{\mathcal{S}}_b$ and calculated by geometrical relations;
$\boldsymbol{\mathcal{E}}_{bH} = \left\{ \begin{array}{c} E_z \end{array} \right\}_H$ is the vector of intensive variables associated to $\boldsymbol{\mathcal{S}}_b$ and calculated by constitutive relations.
In so doing, the RMVT statement with "a-priori" modeling of the transverse electric displacement D_z takes the following form:

$$\int_V \left(\delta\boldsymbol{\mathcal{E}}_{aG}^T\,\boldsymbol{\mathcal{S}}_{aH} + \delta\boldsymbol{\mathcal{E}}_{bG}^T\,\boldsymbol{\mathcal{S}}_b^k + \delta\boldsymbol{\mathcal{S}}_b^T\,(\boldsymbol{\mathcal{E}}_{bG} - \boldsymbol{\mathcal{E}}_{bH})\right) dV = \delta L_e. \tag{10}$$

In the next section, the constitutive relations are obtained for the RMVT-D_z variational statement, both in traditional notation, according with Eq.(9), and in the condensed notation, according with Eq.(10).

III. Constitutive relations

Physical constitutive equations, which are suitable for PVD applications, for the electro-mechanical case reduce to:

$$\begin{aligned} \sigma_{ij} &= C_{ijlm}\epsilon_{lm} - e_{ijl}E_l, \\ D_l &= e_{lij}\epsilon_{ij} + \varepsilon_{lm}E_m, \end{aligned} \tag{11}$$

where standard tensor notation is used and Einstein's summation convention is implied over repeated indices and with: C_{ijlm} = elastic coefficients - Hooke's law; e_{lij} = piezoelectric coefficients; ε_{ij} = permittivity coefficients. Note that $2\epsilon_{ij}$ components in tensorial notation correspond to ϵ_{ij} components in vectorial notation, when $i \neq j$).
Passing from indices to vectors in split form (in-plane and out-of-plane components), constitutive variables become: $\boldsymbol{\sigma}_p$, $\boldsymbol{\sigma}_n$, $\boldsymbol{\epsilon}_p$, $\boldsymbol{\epsilon}_n$, $\boldsymbol{E}_p$, E_n, $\boldsymbol{D}_p$, D_n, where E_n and D_n are scalars.
Eq.(11) can be rewritten:[19]

$$\begin{aligned} \boldsymbol{\sigma}_p &= \boldsymbol{C}_{pp}\boldsymbol{\epsilon}_p + \boldsymbol{C}_{pn}\boldsymbol{\epsilon}_n - \boldsymbol{e}_{pp}^T\boldsymbol{E}_p - \boldsymbol{e}_{np}^T E_n \\ \boldsymbol{\sigma}_n &= \boldsymbol{C}_{pn}^T\boldsymbol{\epsilon}_p + \boldsymbol{C}_{nn}\boldsymbol{\epsilon}_n - \boldsymbol{e}_{pn}^T\boldsymbol{E}_p - \boldsymbol{e}_{nn}^T E_n \\ \boldsymbol{D}_p &= \boldsymbol{e}_{pp}\boldsymbol{\epsilon}_p + \boldsymbol{e}_{pn}\boldsymbol{\epsilon}_n + \boldsymbol{\varepsilon}_{pp}\boldsymbol{E}_p + \boldsymbol{\varepsilon}_{pn}E_n \\ D_n &= \boldsymbol{e}_{np}\boldsymbol{\epsilon}_p + \boldsymbol{e}_{nn}\boldsymbol{\epsilon}_n + \boldsymbol{\varepsilon}_{pn}^T\boldsymbol{E}_p + \varepsilon_{nn}E_n, \end{aligned} \tag{12}$$

where matrices $\boldsymbol{C}_{pp}$, $\boldsymbol{C}_{pn}$, $\boldsymbol{C}_{nn}$, $\boldsymbol{e}_{pp}$, $\boldsymbol{e}_{pn}$, $\boldsymbol{e}_{nn}$, $\boldsymbol{\varepsilon}_{pp}$, $\boldsymbol{\varepsilon}_{pn}$ and ε_{nn} contain the constitutive coefficients in Eq.(11), which are already rotated to the physical reference system and are partitioned so that the in-plane quantities are split from the out-of-plane ones.[21,17]

Variationally consistent constitutive relations must be derived according to Eq.(9). To do that, the system in Eq.(12) is rearranged. First, normal component of electric field is obtained:

$$E_n = \varepsilon_{nn}^{-1}(D_n - \boldsymbol{e}_{np}\boldsymbol{\epsilon}_p - \boldsymbol{e}_{nn}\boldsymbol{\epsilon}_n - \boldsymbol{\varepsilon}_{pn}^T\boldsymbol{E}_p) \tag{13}$$

that is:

$$E_n = -\varepsilon_{nn}^{-1}\boldsymbol{e}_{np}\boldsymbol{\epsilon}_p - \varepsilon_{nn}^{-1}\boldsymbol{e}_{nn}\boldsymbol{\epsilon}_n - \varepsilon_{nn}^{-1}\boldsymbol{\varepsilon}_{pn}^T\boldsymbol{E}_p + \varepsilon_{nn}^{-1}D_n. \tag{14}$$

Substituting Eq.(14) in Eq.(12) and keeping Eq.(14) as last equation, RMVT-D_z constitutive relations are obtained:

$$\begin{aligned}
\boldsymbol{\sigma}_p &= (\boldsymbol{C}_{pp} + \boldsymbol{e}_{np}^T\varepsilon_{nn}^{-1}\boldsymbol{e}_{np})\boldsymbol{\epsilon}_p + (\boldsymbol{C}_{pn} + \boldsymbol{e}_{np}^T\varepsilon_{nn}^{-1}\boldsymbol{e}_{nn})\boldsymbol{\epsilon}_n + (-\boldsymbol{e}_{pp}^T + \boldsymbol{e}_{np}^T\varepsilon_{nn}^{-1}\boldsymbol{\varepsilon}_{pn}^T)\boldsymbol{E}_p + (-\boldsymbol{e}_{np}^T\varepsilon_{nn}^{-1})D_n \\
\boldsymbol{\sigma}_n &= (\boldsymbol{C}_{pn}^T + \boldsymbol{e}_{nn}^T\varepsilon_{nn}^{-1}\boldsymbol{e}_{np})\boldsymbol{\epsilon}_p + (\boldsymbol{C}_{nn} + \boldsymbol{e}_{nn}^T\varepsilon_{nn}^{-1}\boldsymbol{e}_{nn})\boldsymbol{\epsilon}_n + (-\boldsymbol{e}_{pn}^T + \boldsymbol{e}_{nn}^T\varepsilon_{nn}^{-1}\boldsymbol{\varepsilon}_{pn}^T)\boldsymbol{E}_p + (-\boldsymbol{e}_{nn}^T\varepsilon_{nn}^{-1})D_n \\
\boldsymbol{D}_p &= (\boldsymbol{e}_{pp} - \boldsymbol{\varepsilon}_{pn}\varepsilon_{nn}^{-1}\boldsymbol{e}_{np})\boldsymbol{\epsilon}_p + (\boldsymbol{e}_{pn} - \boldsymbol{\varepsilon}_{pn}\varepsilon_{nn}^{-1}\boldsymbol{e}_{nn})\boldsymbol{\epsilon}_n + (\boldsymbol{\varepsilon}_{pp} - \boldsymbol{\varepsilon}_{pn}\varepsilon_{nn}^{-1}\boldsymbol{\varepsilon}_{pn}^T)\boldsymbol{E}_p + (\boldsymbol{\varepsilon}_{pn}\varepsilon_{nn}^{-1})D_n \\
E_n &= -\varepsilon_{nn}^{-1}\boldsymbol{e}_{np}\boldsymbol{\epsilon}_p - \varepsilon_{nn}^{-1}\boldsymbol{e}_{nn}\boldsymbol{\epsilon}_n - \varepsilon_{nn}^{-1}\boldsymbol{\varepsilon}_{pn}^T\boldsymbol{E}_p + \varepsilon_{nn}^{-1}D_n.
\end{aligned} \tag{15}$$

A more compact expression of Eq.(15) can be obtained substituting matrices products with a new set of constitutive coefficients, denoted by the "hat".

$$\begin{aligned}
\boldsymbol{\sigma}_p &= \widehat{\boldsymbol{C}}_{pp}\boldsymbol{\epsilon}_p + \widehat{\boldsymbol{C}}_{pn}\boldsymbol{\epsilon}_n + \widehat{\boldsymbol{e}}_{pp}^T\boldsymbol{E}_p + \widehat{\boldsymbol{e}}_{np}^T D_n \\
\boldsymbol{\sigma}_n &= \widehat{\boldsymbol{C}}_{pn}^T\boldsymbol{\epsilon}_p + \widehat{\boldsymbol{C}}_{nn}\boldsymbol{\epsilon}_n + \widehat{\boldsymbol{e}}_{pn}^T\boldsymbol{E}_p + \widehat{\boldsymbol{e}}_{nn}^T D_n \\
\boldsymbol{D}_p &= \widehat{\boldsymbol{e}}_{pp}\boldsymbol{\epsilon}_p + \widehat{\boldsymbol{e}}_{pn}\boldsymbol{\epsilon}_n + \widehat{\boldsymbol{\varepsilon}}_{pp}\boldsymbol{E}_p + \widehat{\boldsymbol{\varepsilon}}_{pn}D_n \\
E_n &= \widehat{\boldsymbol{e}}_{np}\boldsymbol{\epsilon}_p + \widehat{\boldsymbol{e}}_{nn}\boldsymbol{\epsilon}_n + \widehat{\boldsymbol{\varepsilon}}_{pn}^T\boldsymbol{E}_p + \widehat{\varepsilon}_{nn}D_n.
\end{aligned} \tag{16}$$

Constitutive relations in Eq.(16) are suitable for the application of the RMVT variational statement in the form of Eq.(9).

If the variational statement of Eq.(10) is addressed to, constitutive relations are obtained as it follows, according to the condensed notation.

For sake of clarity, it is convenient to specify that primary unknowns variables are collected in the vector $\boldsymbol{V}^{kT} = \left\{ \begin{array}{ccccc} u_x^k & u_y^k & u_z^k & \phi^k & D_z^k \end{array} \right\}$,

where the superscript k stands for the k-th layer.

It is useful to rewrite vectors introduced in Sec.B:

$\boldsymbol{\mathcal{E}}_a^{kT} = \left\{ \begin{array}{cccccccccc} \epsilon_{xx}^k & \epsilon_{yy}^k & \epsilon_{xy}^k & E_x^k & E_y^k & \epsilon_{zz}^k & \epsilon_{xz}^k & \epsilon_{yz}^k \end{array} \right\}$; $\boldsymbol{\mathcal{E}}_b^{kT} = \left\{ \begin{array}{c} E_z^k \end{array} \right\}$;

$\boldsymbol{\mathcal{S}}_a^{kT} = \left\{ \begin{array}{cccccccccc} \sigma_{xx}^k & \sigma_{yy}^k & \sigma_{xy}^k & -D_x^k & -D_y^k & \sigma_{zz}^k & \sigma_{xz}^k & \sigma_{yz}^k \end{array} \right\}$; $\boldsymbol{\mathcal{S}}_b^{kT} = \left\{ \begin{array}{c} -D_z^k \end{array} \right\}$.

Following geometrical relations can be written:

$$\boldsymbol{\mathcal{E}}_{aG}^k = \boldsymbol{D}_a\boldsymbol{V}^k; \tag{17}$$

$$\boldsymbol{\mathcal{E}}_{bG}^k = \boldsymbol{D}_b\boldsymbol{V}^k; \tag{18}$$

$$\boldsymbol{\mathcal{S}}_{bG}^k = \boldsymbol{D}_{b'}\boldsymbol{V}^k. \tag{19}$$

In explicit form:

$$\boldsymbol{D}_a = \begin{pmatrix} \partial_x & 0 & 0 & 0 & 0 \\ 0 & \partial_y & 0 & 0 & 0 \\ \partial_y & \partial_x & 0 & 0 & 0 \\ 0 & 0 & 0 & -\partial_x & 0 \\ 0 & 0 & 0 & -\partial_y & 0 \\ 0 & 0 & \partial_z & 0 & 0 \\ \partial_z & 0 & \partial_x & 0 & 0 \\ 0 & \partial_z & \partial_y & 0 & 0 \end{pmatrix}; \quad \boldsymbol{D}_b = \begin{pmatrix} 0 & 0 & 0 & -\partial_z & 0 \end{pmatrix}; \quad \boldsymbol{D}_{b'} = \begin{pmatrix} 0 & 0 & 0 & 0 & -1 \end{pmatrix}.$$

Referring to the condensed notation and specifying which quantities are obtained by Hooke's law or by geometrical relations, Eq.(16) becomes:

$$\widetilde{\boldsymbol{\mathcal{S}}}^k_H = \widetilde{\boldsymbol{H}}^k \widetilde{\boldsymbol{\mathcal{E}}}^k_G. \tag{20}$$

$\tilde{\boldsymbol{\mathcal{S}}}^k_H$ is composed by the vector of not modeled extensive variables $\boldsymbol{\mathcal{S}}^k_{aH}$ and the vector of intensive variables $\boldsymbol{\mathcal{E}}_{bH}$ (which is associated to $\boldsymbol{\mathcal{S}}^k_b$); $\widetilde{\boldsymbol{\mathcal{E}}}^k_G$ is composed by the vector of intensive variables $\boldsymbol{\mathcal{E}}^k_{aG}$ (which is associated to $\boldsymbol{\mathcal{S}}^k_a$) and the vector of modeled extensive variables $\boldsymbol{\mathcal{S}}^k_b$, that can be thought as a geometrical vector, by Eq.(19): $\widetilde{\boldsymbol{\mathcal{S}}}^{kT}_H = \left\{ \begin{array}{cc} \boldsymbol{\mathcal{S}}^{kT}_{aH} & \boldsymbol{\mathcal{E}}^{kT}_{bH} \end{array} \right\}$; $\widetilde{\boldsymbol{\mathcal{E}}}^{kT}_G = \left\{ \begin{array}{cc} \boldsymbol{\mathcal{E}}^{kT}_{aG} & \boldsymbol{\mathcal{S}}^{kT}_{bG} \end{array} \right\}$.
The physical constitutive matrix $\boldsymbol{H}^k$ can be partitioned by dividing cells related to modeled and not modeled quantities:

$$\boldsymbol{H}^k = \left\{ \begin{array}{cc} \boldsymbol{H}^k_{aa} & \boldsymbol{H}^k_{ab} \\ \boldsymbol{H}^k_{ba} & \boldsymbol{H}^k_{bb} \end{array} \right\}, \tag{21}$$

where $\boldsymbol{H}^k_{ab} = \boldsymbol{H}^{kT}_{ba}$.
In explicit form:

$$\boldsymbol{H}^k_{aa} = \begin{pmatrix} C^k_{11} & C^k_{12} & C^k_{16} & 0 & 0 & C^k_{13} & 0 & 0 \\ C^k_{12} & C^k_{22} & C^k_{26} & 0 & 0 & C^k_{23} & 0 & 0 \\ C^k_{16} & C^k_{26} & C^k_{66} & 0 & 0 & C^k_{36} & 0 & 0 \\ 0 & 0 & 0 & -\varepsilon^k_{11} & -\varepsilon^k_{12} & 0 & 0 & 0 \\ 0 & 0 & 0 & -\varepsilon^k_{12} & -\varepsilon^k_{22} & 0 & 0 & 0 \\ C^k_{13} & C^k_{23} & C^k_{36} & 0 & 0 & C^k_{33} & 0 & 0 \\ 0 & 0 & 0 & 0 & 0 & 0 & C^k_{55} & C^k_{45} \\ 0 & 0 & 0 & 0 & 0 & 0 & C^k_{45} & C^k_{44} \end{pmatrix}; \quad \boldsymbol{H}^k_{ab} = \begin{pmatrix} -e^k_{31} \\ -e^k_{32} \\ -e^k_{36} \\ 0 \\ 0 \\ -e^k_{33} \\ 0 \\ 0 \end{pmatrix};$$

$$\boldsymbol{H}^k_{ba} = \begin{pmatrix} -e^k_{31} & -e^k_{32} & -e^k_{36} & 0 & 0 & -e^k_{33} & 0 & 0 \end{pmatrix}; \quad \boldsymbol{H}^k_{bb} = \begin{pmatrix} -\varepsilon^k_{33} \end{pmatrix}.$$

Physical constitutive relations, can be arranged according to the above partitioning:

$$\boldsymbol{\mathcal{S}}^k_{aH} = \boldsymbol{H}^k_{aa}\boldsymbol{\mathcal{E}}^k_{aG} + \boldsymbol{H}^k_{ab}\boldsymbol{\mathcal{E}}^k_{bG}, \quad \boldsymbol{\mathcal{S}}^k_{bH} = \boldsymbol{H}^k_{ba}\boldsymbol{\mathcal{E}}^k_{aG} + \boldsymbol{H}^k_{bb}\boldsymbol{\mathcal{E}}^k_{bG}. \tag{22}$$

From Eqs.(22) one has:

$$\boldsymbol{\mathcal{S}}^k_{aH} = \widetilde{\boldsymbol{H}}^k_{aa}\boldsymbol{\mathcal{E}}^k_{aG} + \widetilde{\boldsymbol{H}}^k_{ab}\boldsymbol{\mathcal{S}}^k_{bG}, \quad \boldsymbol{\mathcal{E}}^k_{bH} = \widetilde{\boldsymbol{H}}^k_{ba}\boldsymbol{\mathcal{E}}^k_{aG} + \widetilde{\boldsymbol{H}}^k_{bb}\boldsymbol{\mathcal{S}}^k_{bG}, \tag{23}$$

with:

$$\widetilde{\boldsymbol{H}}^k_{aa} = \boldsymbol{H}^k_{aa} - \boldsymbol{H}^k_{ab}(\boldsymbol{H}^k_{bb})^{-1}\boldsymbol{H}^k_{ba}; \quad \widetilde{\boldsymbol{H}}^k_{ab} = \boldsymbol{H}^k_{ab}(\boldsymbol{H}^k_{bb})^{-1}; \quad \widetilde{\boldsymbol{H}}^k_{ba} = -(\boldsymbol{H}^k_{bb})^{-1}\boldsymbol{H}^k_{ba}; \quad \widetilde{\boldsymbol{H}}^k_{bb} = (\boldsymbol{H}^k_{bb})^{-1}.$$

Matrix $\widetilde{\boldsymbol{H}}^k$ of Eq.(20) is:

$$\widetilde{\boldsymbol{H}}^k = \left\{ \begin{array}{cc} \widetilde{\boldsymbol{H}}^k_{aa} & \widetilde{\boldsymbol{H}}^k_{ab} \\ \widetilde{\boldsymbol{H}}^k_{ba} & \widetilde{\boldsymbol{H}}^k_{bb} \end{array} \right\}. \tag{24}$$

To be noticed that matrix $\widetilde{\boldsymbol{H}}^k$ represents the constitutive relations suitable for the RMVT-D_z in the form of Eq.(10) and it contains the same information of the system in Eq.(16). See the Appendix A for the explicit form of $\widetilde{\boldsymbol{H}}^k$.
The advantage of using the condensed notation is that the above showed procedure to calculate constitutive relations is applicable also when different/more extensive variables are modeled through the thickness plate z-direction and then it represents a general and an automatic way to calculate the constitutive coefficients for many different cases of variational statements.[20]

IV. Through-the-thickness assumptions of primary variables via CUF

In the framework of the CUF,[22] the primary unknowns are assumed by using a generalized expansion:

$$\boldsymbol{V}^k(x,y,z) = F_\tau(z)\ \boldsymbol{V}^k_\tau(x,y) \quad \tau = 0,1,...,N. \tag{25}$$

The repeated indexes are summed over their ranges. The polynomials $F_\tau(z)$ constitute a set of independent functions. Such base is arbitrarily chosen: power of z, Lagrange polynomials or a combination of Legendre polynomials can be considered. N denotes the order of the introduced expansion. In case of RMVT-D_z application, variables concerning displacements, electrical potential and transverse electric displacement are included in vector $\boldsymbol{V}^k$.
It is understood that, by the arbitrary choice of the thickness expansion, the same computational code can address not just one finite element, but a complete family of them, with different descriptions for primary unknowns along the thickness of the structure. In so doing, the CUF reduces a three-dimensional problem to a two-dimensional problem. Meanwhile, the order of the expansion along the thickness of the plate is taken as a free parameter of the finite element and, in the developed code, it can be changed ranging from 1 up to 4.
By appropriately choosing the thickness functions, both an Equivalent Single Layer (ESL) and Layer Wise (LW) description along the thickness of the plate is admissible. In an ESL model, a global assumption for the unknowns is considered along the thickness of the plate (i.e. a Taylor expansion) while, in a LW model, the expansion is made for each layer separately and then interlaminar continuity conditions are enforced by the assembly procedure. The latter leads generally to more accurate results but the number of the nodal degrees of freedom increases with the number of the layers coming out to a greater computational cost.
In the implemented code, for a LW theory the thickness functions are defined by:

$$F_t = \frac{P_0 + P_1}{2}, \quad F_b = \frac{P_0 - P_1}{2}, \quad F_r = P_r - P_{r-2} \quad r = 2,\dots,N, \tag{26}$$

where $P_i = P_i(\zeta_k)$ is the *Legendre* polynomial of i-th order defined in the domain $-1 \le \zeta_k \le 1$. The chosen thickness functions have the interesting properties:

$$\zeta_k = \begin{cases} 1: & F_t = 1, \quad F_b = 0, \quad F_r = 0 \\ -1: & F_t = 0, \quad F_b = 1, \quad F_r = 0 \end{cases}. \tag{27}$$

Using these definitions, the generalized assumptions for the primary unknowns of the k-th layer in Eq.(25) can be stated as:

$$\boldsymbol{V}^{\,k}(x,y,z) = F_b(z)\boldsymbol{V}^{\,k}_{\,b}(x,y) + F_r(z)\boldsymbol{V}^{\,k}_{\,r}(x,y) + F_t(z)\boldsymbol{V}^{\,k}_{\,t}(x,y) = F_\tau\,\boldsymbol{V}^{\,k}_{\,\tau}, \quad \text{with} \quad r = 2,\dots,N. \tag{28}$$

The variables $\boldsymbol{V}_{\,b}$ and $\boldsymbol{V}_{\,t}$ are the actual primary unknowns at the bottom and the top surfaces of the layer and the inter-laminar continuity can be easily imposed:

$$\boldsymbol{V}^{\,k}_{\,t} = \boldsymbol{V}^{\,(k+1)}_{\,b}, \quad \text{with} \quad k = 1,\dots,N_l - 1. \tag{29}$$

Acronyms are used for the implemented plate elements. These are denoted by LM1, LM2, LM3, LM4 in which: L states that a Layer-Wise description is employed and M indicates that mixed approach based on RMVT is used; 1-4 denotes the order of the expansion introduced for the field variables in each layer (from first to fourth order). When acronyms EM1, EM2, EM3, EM4 are used, an Equivalent-Single-Layer description is employed. LD1, LD2, LD3, LD4 and ED1, ED2, ED3, ED4 are the corresponding acronyms when classical approach based on PVD is used (letter D).

V. "Fundamental Nuclei" and FE matrices

This section is devoted to the RMVT-D_z variational statement, while the application of the corresponding PVD has been already illustrated.[20]

A. Finite element discretization

In case of FEM implementation, unknowns can be expressed in terms of their nodal values, via the shape functions N_i:

$$\boldsymbol{V}_{\tau}^{k}(x,y) = N_i(x,y)\boldsymbol{R}_{\tau i}^{k} \quad i = 1,2,...,N_n, \tag{30}$$

while for the virtual variations:

$$\delta\boldsymbol{V}_{s}^{k}(x,y) = N_j(x,y)\delta\boldsymbol{R}_{sj}^{k} \quad j = 1,2,...,N_n, \tag{31}$$

where N_n denotes the number of nodes concerning the considered finite element and $\boldsymbol{R}_{\tau i}^{k}$ is the vector containing nodal values of unknowns:

$$\boldsymbol{R}_{\tau i}^{kT} = \left\{ \begin{array}{ccccc} R_{u_1\tau i}^{k} & R_{u_2\tau i}^{k} & R_{u_3\tau i}^{k} & R_{\phi\tau i}^{k} & R_{D_3\tau i}^{k} \end{array} \right\}. \tag{32}$$

The final expression of the unknowns is:

$$\boldsymbol{V}^{k}(x,y,z) = F_{\tau}N_i\boldsymbol{R}_{\tau i}^{k}. \tag{33}$$

B. Derivation of Fundamental Nuclei and FE matrices

Upon substitution of Eqs.(17), (18), (19), (23) and (31), the variational statement in Eq.(10) leads to a set of equilibrium equations which can be formally put in the following compact form:

$$\delta\boldsymbol{R}_{sj}^{k}: \quad \boldsymbol{K}^{k\tau sij}\,\boldsymbol{R}_{\tau i}^{k} \;=\; \boldsymbol{P}_{sj}^{k}, \tag{34}$$

where $\boldsymbol{P}^{k}$ is the vector of nodal loads and the related boundary conditions are $\overline{\boldsymbol{R}}^{k}$.
The number of obtained equations coincides with the number of introduced variables: τ and s vary from 0 to N, i and j vary from 1 to N_n and k ranges from 1 to N_l.
Matrix $\boldsymbol{K}^{k\tau sij}$ is the fundamental nucleus. In this case it is a 5×5 array and, more in general, it provides the information to build the stiffness matrix (see the Appendix A for the explicit form of $\boldsymbol{K}^{k\tau sij}$).
Whatever is the considered variational statement, starting from the fundamental nucleus, for a given discretization, the stiffness matrix $\boldsymbol{K}$ can be calculated by numerical integration and the assembly procedure. $\boldsymbol{K}$ is representative of the Gibbs free energy contribution and it should be emphasized that, regardless its name, the stiffness matrix contains information pertaining to all the considered fields and not just to the mechanical field. If a static analysis is required, the system to solve is the following:

$$\boldsymbol{K}\boldsymbol{R} = \boldsymbol{P}. \tag{35}$$

where:
$\boldsymbol{P}$ is the vector of nodal loads;
$\boldsymbol{R}$ is the vector of nodal unknowns.

VI. Numerical results and discussion

In this section a few FEM results are compared with the corresponding RMVT-D_z analytical solution (with fourth order through the thickness expansion) and with the exact solution provided by Heyliger.[23] Present case study is also illustrated in a previous paper,[24] where comparisons with the analytical solutions are missing. They are considered in this work.

A three layer thin square plate of unitary side ($a = 1$ $[m]$) loaded by a sinusoidal unitary pressure at the top face ($\widehat{p}_z = 1$ $[N/m^2]$) is considered in the following mechanical assessment. The plate is simply supported at the two opposite sides with zero pressure (cylindrical bending). The layers are of equal thickness and they are made of the same orthotropic material. The total thickness ratio is $a/h = 100$ and the lamination scheme is [0/90/0]. Material properties are: $E_1 = 25$, $E_2 = 1$, $E_3 = 1$, $G_1 = 0.5$, $G_2 = 0.5$, $G_3 = 0.2$ (all in $[GPa]$); $\nu_{12} = 0.25$, $\nu_{13} = 0.25$, $\nu_{25} = 0.25$. Since the plate is very thin, the reduced integration technique has been preserved in order to overcome the shear locking phenomena. Convergence results concerning the midplane transverse displacement at the center of the plate are shown in Fig.1 for LMn and EDn Q4 FEs (Q4

stands for four-nodes Quadrangular finite elements). Regular $n \times 1$ meshes are considered. Following remark can be made. LMn FEs have good convergency properties. It can be noticed that, even when calculating a displacement, simple FEs like ED1 and ED2 converge to a value different from the 3D solution. Such difference decreases as the order of the thickness expansion increases. The obtained convergence properties are preserved for electrical quantities, when piezoelectric materials are included in the lamination. For sake of conciseness this analysis is not quoted.

A simply supported cross-ply [0/90] laminate composed of an elastic material with piezoelectric layers bonded to the upper and lower surfaces is considered for the following electromechanical case study. The elastic layer of the [0] fiber-angle is on the top. The plate is square with a side length a. The total thickness is h. The elastic layers have a thickness of $0.4h$, while the thickness of the piezoelectric layers is $0.1h$. The plate aspect ratio is $a/h = 4$. The elastic material is modeled as a fiber-reinforced composite and has the properties $E_{11} = 132.38$ (all in $[GPa]$), $E_{22} = 10.756$, $E_{33} = 10.756$, $G_{44} = 3.606$, $G_{55} = 5.654$, $G_{66} = 5.654$, $\nu_{12} = 0.24$, $\nu_{13} = 0.24$, $\nu_{23} = 0.49$, $\varepsilon_{11}/\varepsilon_0 = 3.5$, and $\varepsilon_{22}/\varepsilon_0 = \varepsilon_{33}/\varepsilon_0 = 3.0$. The material of the piezoelectric layers is PZT-4 and the material properties are $E_{11} = E_{22} = 81.3$ (all in $[GPa]$), $E_{33} = 64.5$, $G_{44} = G_{55} = 25.6$, $G_{66} = 30.6$, $\nu_{12} = 0.329$, $\nu_{13} = \nu_{23} = 0.432$, $e_{31} = e_{32} = -5.20$ (all in $[C/m^2]$), $e_{33} = 15.08$, $e_{24} = e_{15} = 12.72$, and $\varepsilon_{11}/\varepsilon_0 = \varepsilon_{11}/\varepsilon_0 = 1475$, $\varepsilon_{33}/\varepsilon_0 = 1300$. The piezoelectric layer thickness is taken as 0.1 $[m]$. Both the sensor case and actuator case are considered in the following, where p_z indicates a pressure $[N/m^2]$ and ϕ_t indicates the potential $[V]$ imposed on the top face and $\widehat{p}_z = \widehat{\phi}_t = 1$, see Fig.2. The analysis will be restricted to LW cases. These last are, in fact, capable to furnish reliable results at each layer interface. A second order thickness expansion is considered to properly calculate the through-the-thickness electric displacement, which clearly shows a parabolic-like trend through the external layers (see Fig.3). For each case, the corresponding LW RMVT-D_z analytical solutions with fourth order thickness expansion is provided too (LM4, analytical).

A. Sensor case

The applied double sinusoidal pressure loading p_z is considered on the top plate surface (sensor configuration). The load amplitude is equal to 1 $[N/m^2]$. The top and bottom laminate surfaces are fixed at zero potential. The FEM results are obtained with a regular 10×10 mesh of LD2 (or LM2) Q4 FEs to minimize computational costs keeping a good accuracy. The exact midplane transverse displacement at the center of the plate is 30.027E-11 $[m]$, while for the LM4 analytical solution is 30.029E-11 $[m]$. The value calculated by the LD2 or LM2 FEs is 30.119E-11 $[m]$. Additional comparisons between the exact solution[25] and the FEM results are shown in Tabs.1-3

A comparison between the 3D-exact solution, PVD and RMVT-D_z results is provided in Tab.1 for displacement u_2 and for the electric potential ϕ: the PVD and RMVT-D_z results are very close and they are in good agreement with the exact solution. In other words, when D_z is modeled by RMVT, the calculated primary variables do not change significantly with respect to PVD. However, if a slight difference is detected, the RMVT results are closer to the exact solution.

A comparison between the 3D-exact solution, PVD and RMVT-D_z results is provided in Tab.2 for the transverse stress σ_{33} and for the in-plane stresses σ_{22} and σ_{12}: the PVD and RMVT-D_z results are close to the exact solutions. It has been confirmed that, even for stresses, the difference between PVD and RMVT-D_z is negligible.

The advantages of RMVT-D_z implementation are evident in Tab.3, where the evaluation of transverse displacement is referred to. The results are compared with 3D-exact and to PVD solutions. It should be underlined that RMVT-D_z leads to an almost 3D-exact description, while PVD results can be affected by very large errors (see also Fig.3). In the RMVT-D_z* column, the D_z is calculated by using the physical constitutive relations in the RMVT-D_z analysis. It can be noted that the RMVT-D_z* results are very close to the PVD ones.

The charge Q, calculated on the top surface of the top layer of the plate, under plate surface integration of D_z, according to Eq.(1), is shown in Tab.4. It is important to underline that RMVT-D_z provides a different charge value from PVD (almost 15% different) and this would encourage the use of RMVT-D_z, which appears mandatory the sensor case.

B. Actuator case

The applied double sinusoidal potential ϕ is considered in the top plate surface (actuator configuration). The load amplitude is equal to 1 $[V]$. The bottom laminate surfaces is fixed at zero potential. The FEM results are obtained with a regular 10×10 mesh of LD2 (or LM2) Q4 FEs. The exact midplane transverse displacement at the center of the plate is -14.711×10^{-12} $[m]$, while the value calculated by the LD2 and LM2 FEs are -14.151×10^{-12} $[m]$ and -14.152×10^{-12} $[m]$, respectively. Other comparisons between the exact solution[25] and the FEM results are shown in Tabs.5-7.
The following remarks can be made. Tab.5 shows that the primary variables, u_2 and ϕ, calculated by FEM are in good agreement with the exact solution provided by Heyliger.[25] As far as Tab.6 is concerned, the in-plane stresses are also calculated with good accuracy, while the normal stress does not have reasonable values around the top and the bottom face of the plate. It is clear, from Tab.7, that the RMVT-D_z modeling, compared to the PVD modeling, does not significantly improve the solution for the actuator case.

C. Shell problems

In this section the shell problems for which 3D solution were given by Bhaskar and Varadan[26] for the pure mechanical problem has been extended to piezoelectric case. The problem has been already referred to assess Unified formulation in both PVD and RMVT for pure mechanical problems.[27] Piezoelectric shells are build by replacing and/or adding piezoelectric layers to the original shells.
The cylindrical shell considered by Bhaskar and Varadan has the following geometry, see Fig.4: $a = 40$, $b = 62.8318853$, $R_\alpha = \infty$, $R_\beta = 10$ and $m = 1$, $n = 8$. The following two lay-outs are considered:
-one piezoelectric layer;
-four layers: two external made by piezoelectric materials, and two internal are carbon fiber cross ply $(0/90)$.
Mechanical properties are those used in the plate case. Both actuator and sensor configurations are treated. For the actuator case the distribution of electric potential Φ applied at top surface is

$$\Phi(\alpha, \beta) = \overline{\Phi} sin(\frac{\pi\alpha}{a}) \sin(\frac{8\pi\beta}{b}), \tag{36}$$

with $\overline{\Phi}_{top} = 1$, $\overline{\Phi}_b = 0$ and $\overline{P}_z = 0$.
A mechanical transverse pressure is applied with correspondence to the bottom surface in the sensor case:

$$P_z(\alpha, \beta) = \overline{P}_z sin(\frac{\pi\alpha}{a}) \sin(\frac{8\pi\beta}{b}), \tag{37}$$

with $\overline{\Phi}_{top} = \overline{\Phi}_b = 0$, and $\overline{P}_z = 1$.

Results are given in Tabs.8-11. Different variational statements are compared for thick and thin shells. Electric potential and transverse electric displacement are considered. Three letters acronyms are used to identify the analytical modeling. The first letter "L'' means that LayerWise description is applied; the second letter is "D'' or "M'' in case of PVD modeling or RMVT-D_z modeling, respectively; the subsequent number specifies the employed order for the through-the-thickness expansion of variables. Tabs.8,9 are related to one-layer case. Tabs.10,11 are related to four-layers case. Actuator and sensor configurations are considered, respectively.
Tab.8-11 shows that higher order expansions leads to the same results for both electric potential, even though different variational statements are referred to. Normal electric displacement results related to RMVT applications are quite different with respect to PVD ones (where $\mathcal{D}_z$ is not an assumed variable). These differences are larger for the sensor case: see Tabs.9,11) where a mechanical loading is applied at the bottom of shell.
Concerning Tabs.10,11, which refer to a four-layered configuration, the presence of two mechanical layers reduces the electric coupling. Furthermore, for the sensor case the effect of the radii of curvature is larger than for the actuator one. If the transverse electric displacement is concerned about, the superiority of RMVT with respect to PVD is confirmed, especially for the sensor case.

VII. Conclusions

A new mixed variational statement (RMVT-D_z) is proposed in this work for the "a priori" evaluation of the transverse electric displacement D_z. FE plate elements and corresponding analytical solutions have

been developed to asses the numerical performance of RMVT-D_z. The numerical results clearly show that RMVT-D_z is capable of furnishing almost 3D-results for the D_z. For the sensor case, worse evaluations of D_z are instead obtained by using other variational statements, which discard the interlaminar continuity of D_z. In short, the RMVT-D_z should be preferred to other variational statements when fast and accurate results are needed for the prediction of D_z and of the electrical charge Q on the plate. Future work could be devoted to consider additional lay-out, boundary conditions and load cases.

VIII. Acknowledgements

This work has been carried out with the partial support of European Space Agency, ESTEC-Contract No. 21082/06/NL/PA.

References

[1]D.A. Saravanos and P.R. Heyliger. Mechanics and computational models for laminated piezoelectric beams, plates, and shell. *Applied Mechanic Review*, 52(10):305–320, 1999.

[2]Ji Wang and Jiashi Yang. High-order theories of pieoelectric plates and applications. *Applied Mechanis Review*, 53(4):87–96, 2000.

[3]A.H. Sheikh, P. Topdar, and S. Halder. An appropriate fe model for through-thickness variation of displacement and potential in thin moderately thick smart laminates. *Composite Structutres*, 51:401–409, 2001.

[4]F. Auricchio, P. Bisegna, and C. Lovadina. Finite element approximation of piezoelectric plates. *International Journal for Numerical Methods in Engineering*, 50:1469–1499, 2001.

[5]R.P. Thornbuegh and A. Chattopadhyay. Simultaneous modeling of mechanical and electrical response of smart composite structures. *AIAA Journal*, 40(8):1603–1610, 2002.

[6]Xiaoping Shu. Free-vibration of laminated piezoelectric composite plates based on an accurate theory. *Composite Structures*, 67:375–382, 2005.

[7]Jinho Oh and Maenghyo Cho. A finite element based on cubic zig-zag plate theory for the prediction of thermo-electric-mechanical behaviors. *International Journal of Solids and Structures*, 2004.

[8]M. Kogl and M.L. Bucalem. Analysis of smart laminates using piezoelectric mitc plate and shell elements. *Computers and Structures*, 83:1153–1163, 2005.

[9]M. Kogl and M.L. Bucalem. A family of piezoelectric mitc plate elements. *Computers and Structures*, 83:1277–1297, 2005.

[10]E. Carrera. c_z^0 requirements - models for the two dimensional analysis of multilayered structures. *Composite Structures*, 37:373–383, 1997.

[11]E. Reissner. On a certain mixed variational theory and a proposed application. *International journal for Numerical Methods in Engineering*, 20:1366–1368, 1984.

[12]E. Reissner. On a mixed varational theorem and on shear deformable plate theory. *International journal for Numerical Methods in Engineering*, 23:193–198, 1986.

[13]E. Carrera. c^o reissner-mindlin multilayered plate elements including zig-zag and interlaminar stresses continuity. *International Journal Numerical Methods in Engineering*, 39:1797–1820, 1996.

[14]L. DeMasi E. Carrera. Classical and advanced multilayered plate elements based upon pvd and rmvt. part 1. derivation of finite element matrice. *International Journal Numerical Methods in Engineering*, 55:191–231, 2002.

[15]E. Carrera. Theories and finite elements for multilayered plates and shells: a unified compact formulation with numerical assessment and benchmarking. *Archives of Computational Methods in Engineering*, 10:215–297, 2003.

[16]R.Garcia Lage, C.M. Mota Soares, C.A. Mota Soares, and J.N. Reddy. Modeling of piezoelaminated plates using layerwise mixed finite elements. *Computers and Structures*, 82:1849–1863, 2004.

[17]M. D'Ottavio and B. Kröplin. An extension of reissner mixed variational theorem to piezoelectric laminates. *Mechanics of Advanced Materials and Structures*, 13(2):139–150, 2006.

[18]E. Carrera and M. Boscolo. Classical and mixed finite elements for static and dynamics analysis of piezoelectric plates. *International Journal Numerical Methods in Engineering*, 70:253–291, 2007.

[19]E. Carrera and C. Fagiano. Mixed piezoelectric plate elements with continuous transverse electric displacements. *Journal of Mechanics of Materials and Structures*, 2(3):421–438, 2007.

[20]E. Carrera, S. Brischetto, and P. Nali. Variational statements and computational models for multifield problems and multilayered structures. *Special Issue of MAMS*, 15(3):182–198, 2008.

[21]D. Sc. Nellya L. Rogacheva. The theory of piezoelectric shells and plates. *CRC press*, 1998.

[22]E. Carrera. An assessment of mixed and classical theories for the thermal stress analysis of orthotropic multilayered plates. *Journal of Thermal Stress*, 23:797–831, 2000.

[23]P. Heyliger and D.A. Saravanos. Exact free-vibration analysis of laminated plates with embedded piezoelectric layers. *Journal of Acoustical Society of America*, 98(3):1547–1557, 1995.

[24]E. Carrera, P. Nali, Mixed Piezoelectric Plate Elements with Direct Evaluation of Transverse Electric Displacement, International Journal for Numerical Methods in Engineering, in press.

[25]P. Heyliger. Static behavior of laminated elastic-piezoelectric plates. *AIAA Journal*, 32(12):2481–2484, 1994.

[26]T.K. Varadan, K. Bhaskar, Bending of laminated orthotropic cylindrical shells, Composite Structures 17 (1991) 141–156.

[27]E. Carrera, Multilayered shell theories accounting for layerwise mixed description. Part 1: governing equations; Part 2: numerical evaluations, AIAA Journal 37 (9) (1999) 1107–1124.

A. Appendix: Explicit forms of RMVT-D_z Fundamental Nuclei

The stiffness fundamental nucleus $\boldsymbol{K}^{k\tau sij}$ related to the RMVT-D_z application is listed below. Constitutive information are included too. In the following, the layer-superscript k is always implied to simplify equations.
The stiffness fundamental nucleus is:

$$\boldsymbol{K}^{\tau sij} = \begin{bmatrix} K_{11} & K_{12} & K_{13} & K_{14} & K_{15} \\ K_{21} & K_{22} & K_{23} & K_{24} & K_{25} \\ K_{31} & K_{32} & K_{33} & K_{34} & K_{35} \\ K_{41} & K_{42} & K_{43} & K_{44} & K_{45} \\ K_{51} & K_{52} & K_{53} & K_{54} & K_{55} \end{bmatrix}. \tag{A.38}$$

Its elements are:

$$\begin{aligned}
K_{11} &= \widetilde{\boldsymbol{H}}_{aa}(7,7) \triangleleft N_i N_j \triangleright_{A_k} F_{\tau,z} F_{s,z} + \widetilde{\boldsymbol{H}}_{aa}(1,1) \triangleleft N_{i,x} N_{j,x} \triangleright_{A_k} F_\tau F_s + \widetilde{\boldsymbol{H}}_{aa}(3,1) \triangleleft N_{i,y} N_{j,x} \triangleright_{A_k} F_\tau F_s + \\
&\quad + \widetilde{\boldsymbol{H}}_{aa}(1,3) \triangleleft N_{i,x} N_{j,y} \triangleright_{A_k} F_\tau F_s + \widetilde{\boldsymbol{H}}_{aa}(3,3) \triangleleft N_{i,y} N_{j,y} \triangleright_{A_k} F_\tau F_s; \\
K_{21} &= \widetilde{\boldsymbol{H}}_{aa}(8,7) \triangleleft N_i N_j \triangleright_{A_k} F_{\tau,z} F_{s,z} + \widetilde{\boldsymbol{H}}_{aa}(3,1) \triangleleft N_{i,x} N_{j,x} \triangleright_{A_k} F_\tau F_s + \widetilde{\boldsymbol{H}}_{aa}(2,1) \triangleleft N_{i,y} N_{j,x} \triangleright_{A_k} F_\tau F_s + \\
&\quad + \widetilde{\boldsymbol{H}}_{aa}(3,3) \triangleleft N_{i,x} N_{j,y} \triangleright_{A_k} F_\tau F_s + \widetilde{\boldsymbol{H}}_{aa}(2,3) \triangleleft N_{i,y} N_{j,y} \triangleright_{A_k} F_\tau F_s; \\
K_{31} &= \widetilde{\boldsymbol{H}}_{aa}(7,7) \triangleleft N_{i,x} N_j \triangleright_{A_k} F_\tau F_{s,z} + \widetilde{\boldsymbol{H}}_{aa}(8,7) \triangleleft N_{i,y} N_j \triangleright_{A_k} F_\tau F_{s,z} + \widetilde{\boldsymbol{H}}_{aa}(6,1) \triangleleft N_i N_{j,x} \triangleright_{A_k} F_{\tau,z} F_s + \\
&\quad + \widetilde{\boldsymbol{H}}_{aa}(6,3) \triangleleft N_i N_{j,y} \triangleright_{A_k} F_{\tau,z} F_s; \\
K_{41} &= -\widetilde{\boldsymbol{H}}_{aa}(4,7) \triangleleft N_{i,x} N_j \triangleright_{A_k} F_\tau F_{s,z} - \widetilde{\boldsymbol{H}}_{aa}(5,7) \triangleleft N_{i,y} N_j \triangleright_{A_k} F_\tau F_{s,z}; \\
K_{51} &= \widetilde{\boldsymbol{H}}_{ba}(1,1) \triangleleft N_i N_{j,x} \triangleright_{A_k} F_\tau F_s + \widetilde{\boldsymbol{H}}_{ba}(1,3) \triangleleft N_i N_{j,y} \triangleright_{A_k} F_\tau F_s; \\
K_{12} &= \widetilde{\boldsymbol{H}}_{aa}(7,8) \triangleleft N_i N_j \triangleright_{A_k} F_{\tau,z} F_{s,z} + \widetilde{\boldsymbol{H}}_{aa}(1,3) \triangleleft N_{i,x} N_{j,x} \triangleright_{A_k} F_\tau F_s + \widetilde{\boldsymbol{H}}_{aa}(3,3) \triangleleft N_{i,y} N_{j,x} \triangleright_{A_k} F_\tau F_s + \\
&\quad + \widetilde{\boldsymbol{H}}_{aa}(1,2) \triangleleft N_{i,x} N_{j,y} \triangleright_{A_k} F_\tau F_s + \widetilde{\boldsymbol{H}}_{aa}(3,2) \triangleleft N_{i,y} N_{j,y} \triangleright_{A_k} F_\tau F_s; \\
K_{22} &= \widetilde{\boldsymbol{H}}_{aa}(8,8) \triangleleft N_i N_j \triangleright_{A_k} F_{\tau,z} F_{s,z} + \widetilde{\boldsymbol{H}}_{aa}(3,3) \triangleleft N_{i,x} N_{j,x} \triangleright_{A_k} F_\tau F_s + \widetilde{\boldsymbol{H}}_{aa}(2,3) \triangleleft N_{i,y} N_{j,x} \triangleright_{A_k} F_\tau F_s + \\
&\quad + \widetilde{\boldsymbol{H}}_{aa}(3,2) \triangleleft N_{i,x} N_{j,y} \triangleright_{A_k} F_\tau F_s + \widetilde{\boldsymbol{H}}_{aa}(2,2) \triangleleft N_{i,y} N_{j,y} \triangleright_{A_k} F_\tau F_s; \\
K_{32} &= \widetilde{\boldsymbol{H}}_{aa}(7,8) \triangleleft N_{i,x} N_j \triangleright_{A_k} F_\tau F_{s,z} + \widetilde{\boldsymbol{H}}_{aa}(8,8) \triangleleft N_{i,y} N_j \triangleright_{A_k} F_\tau F_{s,z} + \widetilde{\boldsymbol{H}}_{aa}(6,3) \triangleleft N_i N_{j,x} \triangleright_{A_k} F_{\tau,z} F_s + \\
&\quad + \widetilde{\boldsymbol{H}}_{aa}(6,2) \triangleleft N_i N_{j,y} \triangleright_{A_k} F_{\tau,z} F_s; \\
K_{42} &= -\widetilde{\boldsymbol{H}}_{aa}(4,8) \triangleleft N_{i,x} N_j \triangleright_{A_k} F_\tau F_{s,z} - \widetilde{\boldsymbol{H}}_{aa}(5,8) \triangleleft N_{i,y} N_j \triangleright_{A_k} F_\tau F_{s,z}; \\
K_{52} &= \widetilde{\boldsymbol{H}}_{ba}(1,3) \triangleleft N_i N_{j,x} \triangleright_{A_k} F_\tau F_s + \widetilde{\boldsymbol{H}}_{ba}(1,2) \triangleleft N_i N_{j,y} \triangleright_{A_k} F_\tau F_s; \\
K_{13} &= \widetilde{\boldsymbol{H}}_{aa}(1,6) \triangleleft N_{i,x} N_j \triangleright_{A_k} F_\tau F_{s,z} + \widetilde{\boldsymbol{H}}_{aa}(3,6) \triangleleft N_{i,y} N_j \triangleright_{A_k} F_\tau F_{s,z} + \widetilde{\boldsymbol{H}}_{aa}(7,7) \triangleleft N_i N_{j,x} \triangleright_{A_k} F_{\tau,z} F_s + \\
&\quad + \widetilde{\boldsymbol{H}}_{aa}(7,8) \triangleleft N_i N_{j,y} \triangleright_{A_k} F_{\tau,z} F_s; \\
K_{23} &= \widetilde{\boldsymbol{H}}_{aa}(3,6) \triangleleft N_{i,x} N_j \triangleright_{A_k} F_\tau F_{s,z} + \widetilde{\boldsymbol{H}}_{aa}(2,6) \triangleleft N_{i,y} N_j \triangleright_{A_k} F_\tau F_{s,z} + \widetilde{\boldsymbol{H}}_{aa}(8,7) \triangleleft N_i N_{j,x} \triangleright_{A_k} F_{\tau,z} F_s + \\
&\quad + \widetilde{\boldsymbol{H}}_{aa}(8,8) \triangleleft N_i N_{j,y} \triangleright_{A_k} F_{\tau,z} F_s; \\
K_{33} &= \widetilde{\boldsymbol{H}}_{aa}(6,6) \triangleleft N_i N_j \triangleright_{A_k} F_{\tau,z} F_{s,z} + \widetilde{\boldsymbol{H}}_{aa}(7,7) \triangleleft N_{i,x} N_{j,x} \triangleright_{A_k} F_\tau F_s + \widetilde{\boldsymbol{H}}_{aa}(8,7) \triangleleft N_{i,y} N_{j,x} \triangleright_{A_k} F_\tau F_s + \\
&\quad + \widetilde{\boldsymbol{H}}_{aa}(7,8) \triangleleft N_{i,x} N_{j,y} \triangleright_{A_k} F_\tau F_s + \widetilde{\boldsymbol{H}}_{aa}(8,8) \triangleleft N_{i,y} N_{j,y} \triangleright_{A_k} F_\tau F_s; \\
K_{43} &= -\widetilde{\boldsymbol{H}}_{aa}(4,7) \triangleleft N_{i,x} N_{j,x} \triangleright_{A_k} F_\tau F_s - \widetilde{\boldsymbol{H}}_{aa}(5,7) \triangleleft N_{i,y} N_{j,x} \triangleright_{A_k} F_\tau F_s - \widetilde{\boldsymbol{H}}_{aa}(4,8) \triangleleft N_{i,x} N_{j,y} \triangleright_{A_k} F_\tau F_s + \\
&\quad - \widetilde{\boldsymbol{H}}_{aa}(5,8) \triangleleft N_{i,y} N_{j,y} \triangleright_{A_k} F_\tau F_s; \\
K_{53} &= \widetilde{\boldsymbol{H}}_{ba}(1,6) \triangleleft N_i N_j \triangleright_{A_k} F_\tau F_{s,z};
\end{aligned}$$

$$K_{14} = -\widetilde{\boldsymbol{H}}_{aa}(7,4) \lhd N_i N_{j,x} \rhd_{A_k} F_{\tau,z} F_s - \widetilde{\boldsymbol{H}}_{aa}(7,5) \lhd N_i N_{j,y} \rhd_{A_k} F_{\tau,z} F_s;$$

$$K_{24} = -\widetilde{\boldsymbol{H}}_{aa}(8,4) \lhd N_i N_{j,x} \rhd_{A_k} F_{\tau,z} F_s - \widetilde{\boldsymbol{H}}_{aa}(8,5) \lhd N_i N_{j,y} \rhd_{A_k} F_{\tau,z} F_s;$$

$$K_{34} = -\widetilde{\boldsymbol{H}}_{aa}(7,4) \lhd N_{i,x} N_{j,x} \rhd_{A_k} F_\tau F_s - \widetilde{\boldsymbol{H}}_{aa}(8,4) \lhd N_{i,y} N_{j,x} \rhd_{A_k} F_\tau F_s - \widetilde{\boldsymbol{H}}_{aa}(7,5) \lhd N_{i,x} N_{j,y} \rhd_{A_k} F_\tau F_s + \\ - \widetilde{\boldsymbol{H}}_{aa}(8,5) \lhd N_{i,y} N_{j,y} \rhd_{A_k} F_\tau F_s;$$

$$K_{44} = \widetilde{\boldsymbol{H}}_{aa}(4,4) \lhd N_{i,x} N_{j,x} \rhd_{A_k} F_\tau F_s + \widetilde{\boldsymbol{H}}_{aa}(5,4) \lhd N_{i,y} N_{j,x} \rhd_{A_k} F_\tau F_s + \widetilde{\boldsymbol{H}}_{aa}(4,5) \lhd N_{i,x} N_{j,y} \rhd_{A_k} F_\tau F_s + \\ + \widetilde{\boldsymbol{H}}_{aa}(5,5) \lhd N_{i,y} N_{j,y} \rhd_{A_k} F_\tau F_s;$$

$$K_{54} = \lhd N_i N_j \rhd_{A_k} F_\tau F_{s,z};$$

$$K_{15} = -\widetilde{\boldsymbol{H}}_{ab}(1,1) \lhd N_{i,x} N_j \rhd_{A_k} F_\tau F_s - \widetilde{\boldsymbol{H}}_{ab}(3,1) \lhd N_{i,y} N_j \rhd_{A_k} F_\tau F_s;$$

$$K_{25} = -\widetilde{\boldsymbol{H}}_{ab}(3,1) \lhd N_{i,x} N_j \rhd_{A_k} F_\tau F_s - \widetilde{\boldsymbol{H}}_{ab}(2,1) \lhd N_{i,y} N_j \rhd_{A_k} F_\tau F_s;$$

$$K_{35} = -\widetilde{\boldsymbol{H}}_{ab}(6,1) \lhd N_i N_j \rhd_{A_k} F_{\tau,z} F_s;$$

$$K_{45} = \lhd N_i N_j \rhd_{A_k} F_{\tau,z} F_s;$$

$$K_{55} = -\widetilde{\boldsymbol{H}}_{bb}(1,1) \lhd N_i N_j \rhd_{A_k} F_\tau F_s.$$

Subscripts after comma indicates derivatives and:

$$\lhd(.....)\rhd_{A_k} = \int_{\Omega_k} (.....) d\Omega.$$

The explicit form of matrices $\widetilde{\boldsymbol{H}}_{aa}$,$\widetilde{\boldsymbol{H}}_{ba}$,$\widetilde{\boldsymbol{H}}_{ab}$ and $\widetilde{\boldsymbol{H}}_{bb}$ is:

$$\widetilde{\boldsymbol{H}}_{aa} = \begin{bmatrix} C_{11}+e_{31}^2/\varepsilon_{33} & C_{12}+e_{31}e_{32}/\varepsilon_{33} & C_{16}+e_{31}e_{36}/\varepsilon_{33} & 0 & 0 & C_{13}+e_{31}e_{33}/\varepsilon_{33} & 0 & 0 \\ C_{12}+e_{31}e_{32}/\varepsilon_{33} & C_{22}+e_{32}^2/\varepsilon_{33} & C_{26}+e_{32}e_{36}/\varepsilon_{33} & 0 & 0 & C_{23}+e_{32}e_{33}/\varepsilon_{33} & 0 & 0 \\ C_{16}+e_{31}e_{36}/\varepsilon_{33} & C_{26}+e_{32}e_{36}/\varepsilon_{33} & C_{66}+e_{36}^2/\varepsilon_{33} & 0 & 0 & C_{36}+e_{33}e_{36}/\varepsilon_{33} & 0 & 0 \\ 0 & 0 & 0 & -\varepsilon_{11} & -\varepsilon_{12} & 0 & -e_{15} & -e_{14} \\ 0 & 0 & 0 & -\varepsilon_{12} & -\varepsilon_{22} & 0 & -e_{25} & -e_{24} \\ C_{13}+e_{31}e_{33}/\varepsilon_{33} & C_{23}+e_{32}e_{33}/\varepsilon_{33} & C_{36}+e_{33}e_{36}/\varepsilon_{33} & 0 & 0 & C_{33}+e_{33}^2/\varepsilon_{33} & 0 & 0 \\ 0 & 0 & 0 & -e_{15} & -e_{25} & 0 & C_{55} & C_{45} \\ 0 & 0 & 0 & -e_{14} & -e_{24} & 0 & C_{45} & C_{44} \end{bmatrix};$$

$$\widetilde{\boldsymbol{H}}_{ab}^T = \begin{bmatrix} e_{31}/\varepsilon_{33} & e_{32}/\varepsilon_{33} & e_{36}/\varepsilon_{33} & 0 & 0 & e_{33}/\varepsilon_{33} & 0 & 0 \end{bmatrix};$$

$$\widetilde{\boldsymbol{H}}_{ba} = \begin{bmatrix} -e_{31}/\varepsilon_{33} & -e_{32}/\varepsilon_{33} & -e_{36}/\varepsilon_{33} & 0 & 0 & -e_{33}/\varepsilon_{33} & 0 & 0 \end{bmatrix};$$

$$\widetilde{\boldsymbol{H}}_{bb} = \begin{bmatrix} -1/\varepsilon_{33} \end{bmatrix}.$$

	$u_2 \times 10^{12}$	$u_2 \times 10^{12}$	$u_2 \times 10^{12}$	$u_2 \times 10^{12}$	$\phi \times 10^1$	$\phi \times 10^1$	$\phi \times 10^1$	$\phi \times 10^1$
Height	$3D^{25}$	*Analytical*	*PVD*	*RMVT-*D_z	$3D^{25}$	*Analytical*	*PVD*	*RMVT-*D_z
1.000	-47.549	-47.552	-45.593	-45.594	0.0000	0.0000	0.0000	0.0000
0.975	-41.425	-41.430	-39.527	-39.528	0.0189	0.0189	0.0181	0.0181
0.950	-35.424	-35.427	-33.567	-33.569	0.0358	0.0358	0.0336	0.0336
0.925	-29.531	-29.536	-27.715	-27.772	0.0488	0.0488	0.0464	0.0464
0.900	-23.732	-23.733	-21.969	-21.970	0.0598	0.0599	0.0567	0.0567
0.800	-10.480	-10.530	-10.058	-10.577	0.0589	0.0589	0.0560	0.0559
0.700	0.1413	0.1394	-0.0836	-0.0836	0.0589	0.0589	0.0560	0.0559
0.600	9.8917	9.9064	9.5104	9.5108	0.0596	0.0596	0.0567	0.0567
0.500	20.392	20.384	18.205	18.206	0.0611	0.0611	0.0583	0.0583
0.400	24.768	24.774	22.149	22.150	0.0634	0.0634	0.0606	0.0605
0.300	29.110	29.110	26.700	26.703	0.0665	0.0665	0.0637	0.0637
0.200	33.819	33.838	31.860	31.863	0.0706	0.0706	0.0677	0.0677
0.100	39.309	39.312	37.628	37.632	0.0756	0.0756	0.0726	0.0726
0.075	44.492	44.498	42.930	42.934	0.0602	0.0602	0.0581	0.0581
0.050	49.772	49.776	48.341	48.346	0.0425	0.0425	0.0411	0.0411
0.025	55.163	55.169	53.863	53.867	0.0224	0.0224	0.0218	0.0218
0.000	60.678	60.682	59.494	59.499	0.0000	0.0000	0.0000	0.0000

Table 1. PVD and RMVT-D_z results: comparison between LD2 and LM2 FEM solutions with the 3D-exact and the analytical LM4 solutions, sensor case. Displacements are in $[m]$; electric potential is in $[V]$. $u_2 = u_2(a/2, 0)$; $\phi = \phi(a/2, b/2)$.

	$\sigma_{33} \times 10^1$	$\sigma_{33} \times 10^1$	$\sigma_{33} \times 10^1$	$\sigma_{33} \times 10^1$	σ_{22}	σ_{22}	σ_{22}	σ_{22}	σ_{12}	σ_{12}	σ_{12}	σ_{12}
Height	$3D^{25}$	*Analytical*	*PVD*	*RMVT-*D_z	$3D^{25}$	*Analytical*	*PVD*	*RMVT-*D_z	$3D^{25}$	*Analytical*	*PVD*	*RMVT-*D_z
1.000	10.000	10.000	9.6313	9.6381	6.5643	6.5642	6.2392	6.2387	-2.4766	-2.4768	-2.3547	-2.3546
0.975	9.9657	9.9645	9.4336	9.4354	5.8201	5.8203	5.5033	5.5030	-2.1824	-2.1827	-2.0680	-2.0679
0.950	9.8682	9.8683	9.3631	9.3598	5.0855	5.0855	4.7857	4.7856	-1.8942	-1.8944	-1.7866	-1.7864
0.925	9.7154	9.7146	9.4197	9.4112	4.3595	4.3597	4.0865	4.0866	-1.6114	-1.6116	-1.5103	-1.5102
0.900	9.5151	9.5177	9.6034	9.5898	3.6408	3.6408	3.4057	3.4059	-1.3332	-1.3333	-1.2393	-1.2392
0.900	9.5151	9.5177	10.163	10.163	2.8855	2.8858	3.8364	3.8362	-0.2463	-0.2464	-0.2290	-0.2290
0.800	8.5199	8.5167	8.7018	8.7018	1.4499	1.4551	2.0094	2.0093	-0.1534	-0.1539	-0.1475	-0.1474
0.700	7.3747	7.3757	7.4395	7.4395	0.2879	0.2880	0.3332	0.3332	-0.0817	-0.0817	-0.0776	-0.0775
0.600	6.1686	6.1683	6.3764	6.3764	-0.7817	-0.7829	-1.1923	-1.1922	-0.0212	-0.0213	-0.0193	-0.0193
0.500	4.9831	4.9817	5.5124	5.5124	-1.9266	-1.9266	-2.5670	-2.5669	0.0369	0.0370	0.0274	0.0274
0.500	4.9831	4.9817	4.9178	4.9179	0.0991	0.0991	0.0527	0.0527	0.0369	0.0370	0.0274	0.0274
0.400	3.8045	3.8049	3.9244	3.9244	-0.0149	-0.0150	-0.0683	-0.0683	0.0965	0.0966	0.0771	0.0771
0.300	2.6137	2.6131	2.8259	2.8259	-0.1280	-0.1281	-0.2049	-0.2049	0.1529	0.1529	0.1335	0.1335
0.200	1.4821	1.4850	1.6223	1.6223	-0.2426	-0.2427	-0.3571	-0.3570	0.2139	0.2142	0.1966	0.1966
0.100	0.4868	0.4867	0.3136	0.3136	-0.3616	-0.3617	-0.5248	-0.5247	0.2882	0.2883	0.2663	0.2663
0.100	0.4868	0.4867	0.8251	0.8365	-4.2348	-4.2349	-3.9325	-3.9325	1.5603	1.5605	1.4415	1.4413
0.075	0.2845	0.2854	0.9872	0.9436	-4.8806	-4.8808	-4.5636	-4.5634	1.8105	1.8108	1.6933	1.6931
0.050	0.1312	0.1311	1.0311	1.0339	-5.5337	-5.5337	-5.2123	-5.2119	2.0651	2.0652	1.9499	1.9498
0.025	0.0340	0.0353	0.9568	0.9553	-6.1951	-6.1953	-5.8785	5.8780	2.3246	2.3249	2.2115	2.2113
0.000	0.0000	0.0000	0.7641	0.7583	-6.8658	-6.8658	-6.5623	-6.5617	2.5899	2.5901	2.4779	2.4777

Table 2. PVD and RMVT-D_z results: comparison between LD2 and LM2 FEM solutions with the 3D-exact and the analytical LM4 solutions, sensor case. Stresses are in $[Pa]$. $\sigma_{33} = \sigma_{33}(a/2, b/2)$; $\sigma_{11} = \sigma_{11}(a/2, b/2)$; $\sigma_{12} = \sigma_{12}(0, 0)$.

	$D_z \times 10^{13}$				
Height	3D[25]	*Analytical*	*RMVT-*D_z	*PVD*	*RMVT-*D_z^*
1.000	160.58	160.58	160.22	239.57	234.38
0.975	149.35	148.93	148.27	204.92	203.62
0.950	117.23	117.23	117.53	161.38	163.98
0.925	66.568	66.243	68.003	108.95	115.44
0.900	-0.3382	-0.3384	-0.3044	47.621	58.008
0.900	-0.3382	-0.3384	-0.3044	-0.2990	-0.3101
0.800	-0.1276	-0.1277	-0.0969	-0.0977	-0.1027
0.700	0.0813	0.0813	0.1064	0.1037	0.1048
0.600	0.2913	0.2914	0.3058	0.3051	0.3123
0.500	0.5052	0.5053	0.5010	0.5065	0.5198
0.500	0.5052	0.5053	0.5010	0.4943	0.4815
0.400	0.7259	0.7262	0.7228	0.7236	0.7165
0.300	0.9563	0.9564	0.9495	0.9529	0.9515
0.200	1.1995	1.2001	1.1812	1.1821	1.1865
0.100	1.4587	1.4590	1.4179	1.4114	1.4215
0.100	1.4587	1.4590	1.4179	-50.162	-58.915
0.075	-58.352	-58.061	-59.178	-105.53	-111.00
0.050	-103.66	-103.66	-103.15	-152.63	-154.82
0.025	-132.40	-132.03	-130.50	-191.45	-190.36
0.000	-142.46	-142.46	-141.23	-222.00	-217.63

Table 3. Comparison between FEM and the analytical LM4 solution, sensor case. LD2 and LM2 FEs are employed for PVD and RMVT case, respectively. The electric displacement is in $[c/m^2]$. $D_z = D_z(a/2, b/2)$. The D_z RMVT-$D_z{}^*$ is calculated by constitutive relations in the RMVT-D_z analysis.

$Q \times 10^{11}(RMVT - D_z)$	$Q \times 10^{11}(PVD)$	$Q \times 10^{11}(RMVT - D_z*)$
10.219	8.8763	8.5457

Table 4. Comparison between PVD and RMVT-D_z results, sensor case. LD2 or LM2 FEs are employed. Q is the charge at the top surface of the top layer and it is expressed in $[c]$. RMVT-D_z* result is computed starting from the D_z calculated by constitutive relations in the RMVT-D_z analysis.

	$u_2 \times 10^{12}$	$u_2 \times 10^{12}$	$u_2 \times 10^{12}$	$u_2 \times 10^{12}$	$\phi \times 10^1$	$\phi \times 10^1$	$\phi \times 10^1$	$\phi \times 10^1$
Height	$3D^{25}$	*Analytical*	*PVD*	*RMVT-D_z*	$3D^{25}$	*Analytical*	*PVD*	*RMVT-D_z*
1.000	-32.764	-32.765	-33.951	-33.951	1.0000	1.0000	1.0000	1.0000
0.975	-23.349	-23.351	-24.377	-24.377	0.9971	0.9971	0.9972	0.9972
0.950	-13.973	-13.974	-14.826	-14.826	0.9950	0.9950	0.9951	0.9951
0.925	-4.6174	-46.180	-5.2983	-5.2977	0.9936	0.9937	0.9936	0.9936
0.900	4.7356	4.7352	4.2064	4.2069	0.9929	0.9929	0.9929	0.9929
0.800	2.9808	2.9902	2.5445	2.5448	0.8415	0.8418	0.8423	0.8422
0.700	1.7346	1.7346	1.2546	1.2548	0.7014	0.7014	0.7011	0.7011
0.600	0.8008	0.8045	0.3368	0.3368	0.5707	0.5709	0.5695	0.5695
0.500	0.0295	0.0297	-0.2091	-0.2091	0.4476	0.4477	0.4473	0.4475
0.400	-0.4404	-0.4395	-0.5745	-0.5745	0.3305	0.3307	0.3310	0.3311
0.300	-0.8815	-0.8811	-0.9518	-0.9517	0.2179	0.2179	0.2177	0.2177
0.200	-1.3206	-1.3207	-1.3409	-1.3408	0.1081	0.1082	0.1073	0.1073
0.100	-1.7839	-1.7834	-1.7419	-1.7418	-0.0001	-0.0001	-0.0001	-0.0001
0.075	-2.0470	-2.0465	-1.9963	-1.9963	-0.00009	-0.00010	-0.00009	-0.00009
0.050	-2.3140	-2.3134	-2.2554	-2.2554	-0.00008	-0.00008	-0.00007	-0.00007
0.025	-2.5856	-2.5850	-2.5191	-2.5191	-0.00004	-0.00004	-0.00004	-0.00004
0.000	-2.8625	-2.8618	-2.7875	-2.7876	0.00000	0.00000	0.00000	0.00000

Table 5. PVD and RMVT-D_z results: comparison between LD2 and LM2 FEM solutions with the 3D-exact and the analytical LM4 solutions, actuator case. Displacements are in $[m]$; electric potential is in $[V]$. $u_2 = u_2(a/2, 0)$; $\phi = \phi(a/2, b/2)$.

	$\sigma_{33} \times 10^1$	$\sigma_{33} \times 10^1$	$\sigma_{33} \times 10^1$	$\sigma_{33} \times 10^1$	σ_{22}	σ_{22}	σ_{22}	σ_{22}	σ_{12}	σ_{12}	σ_{12}	σ_{12}
Height	$3D^{25}$	*Analytical*	*PVD*	*RMVT-D_z*	$3D^{25}$	*Analytical*	*PVD*	*RMVT-D_z*	$3D^{25}$	*Analytical*	*PVD*	*RMVT-D_z*
1.000	0.0000	0.0004	-55.800	-55.419	111.81	111.80	113.28	113.26	-146.03	-146.04	-148.30	-148.30
0.975	-0.8333	-0.8535	-43.279	-43.183	63.736	63.737	66.186	66.175	-100.77	-100.79	-103.03	-103.03
0.950	-2.8471	-2.8401	-28.385	-28.574	15.833	15.836	19.448	19.447	-55.693	-55.697	-57.858	-57.855
0.925	-5.3241	-5.3090	-11.118	-11.592	-32.001	-31.994	-26.932	-26.923	-10.698	-10.702	-12.781	-12.778
0.900	-7.5482	-7.5328	8.5218	-7.7627	-79.865	-79.851	-72.955	-72.935	34.295	34.293	32.198	32.221
0.900	-7.5482	-7.6043	-15.579	-15.581	-51.681	-51.679	-68.096	-68.104	6.3365	6.3360	5.9489	5.9494
0.800	-12.957	-12.867	-11.567	-11.569	-33.135	-33.231	-41.748	-41.753	4.6631	4.6693	4.2950	4.2954
0.700	-15.245	-15.260	-11.713	-11.714	-19.840	-19.840	-21.342	-21.345	3.3247	3.3246	2.9062	2.9064
0.600	-15.510	-15.458	-16.014	-16.016	-9.7737	-9.8104	-6.8792	-6.8808	2.2096	2.2124	1.7823	1.7825
0.500	-14.612	-14.674	-24.473	-24.475	-1.3905	-1.3905	1.6408	1.6397	1.2286	1.2287	0.9237	0.9238
0.500	-14.612	-14.629	-17.335	-17.337	-1.3089	-1.3099	-1.2973	-1.2975	1.2287	1.2287	0.9237	0.9238
0.400	-12.524	-12.490	-12.937	-12.939	-0.5782	-0.5782	-3.3075	-3.3091	0.5227	0.5252	0.3400	0.3401
0.300	-9.2558	-9.602	-9.2086	-9.2096	0.1348	0.1343	5.7883	5.7872	-0.0572	-0.0571	-0.1927	-0.1926
0.200	-5.5018	-5.4940	-6.1487	-6.1495	0.8463	0.8467	1.4314	1.4313	-0.5840	-0.5839	-0.6744	-0.6744
0.100	-1.8733	-1.8958	-3.7579	-3.7583	1.5723	1.5708	2.2270	2.2270	-1.1220	-1.1217	-1.1051	-1.1051
0.100	-0.8733	-1.8698	-3.3555	-2.8333	14.529	14.523	14.007	13.988	-6.0731	-6.0712	-5.9813	-5.9814
0.075	-1.1074	-1.1102	-4.1098	-3.7838	17.801	17.794	17.041	17.030	-7.3455	-7.3436	-7.1917	-7.1918
0.050	-0.5162	-0.5158	-4.3795	-4.2493	21.098	21.089	20.148	20.144	-8.6346	-8.6321	-8.4220	-8.4222
0.025	-0.1351	-0.1397	-4.1645	-4.2299	24.428	24.419	23.328	23.331	-9.9437	-9.9412	-9.6723	-9.6726
0.000	0.0000	0.0003	-3.4647	-3.7256	27.795	27.778	26.581	26.591	-11.276	-11.273	-10.942	-10.943

Table 6. PVD and RMVT-D_z results: comparison between LD2 and LM2 FEM solutions with the 3D-exact and the analytical LM4 solutions, actuator case. Stresses are in $[Pa]$. $\sigma_{33} = \sigma_{33}(a/2, b/2)$; $\sigma_{11} = \sigma_{11}(a/2, b/2)$; $\sigma_{12} = \sigma_{12}(0, 0)$.

	$D_z \times 10^{13}$			
Height	*Analytical*	*RMVT-*D_z	*PVD*	*RMVT-*D_z^*
1.000	-2.4184	-2.4431	-2.4382	-2.4385
0.975	-1.8220	-1.8416	-1.8388	-1.8388
0.950	-1.2275	-1.2408	-1.2395	-1.2394
0.925	-6.3446	-6.4070	-6.4043	-6.4007
0.900	-4.1874	-4.1321	-4.1504	-4.0924
0.900	-4.1874	-4.1321	-4.1274	-4.1294
0.800	-3.8633	-3.8746	-3.8751	-3.8757
0.700	-3.5886	-3.6205	-3.6228	-3.6220
0.600	-3.3640	-3.3700	-3.3705	-3.3682
0.500	-3.1824	-3.1229	-3.1182	-3.1145
0.500	-3.1824	-3.1229	-3.1275	-3.1313
0.400	-3.0453	-3.0498	-3.0492	-3.0515
0.300	-2.9472	-2.9732	-2.9709	-2.9718
0.200	-2.8902	-2.8931	-2.8925	-2.8920
0.100	-2.8701	-2.8095	-2.8142	-2.8123
0.100	-2.8701	-2.8095	-2.8425	-2.8823
0.075	-2.8384	-2.8409	-2.8144	-2.8393
0.050	-2.8140	-2.8384	-2.7898	-2.7997
0.025	-2.7990	-2.8020	-2.7685	-2.7635
0.000	-2.7934	-2.7316	-2.7507	-2.7307

Table 7. Comparison between FEM and the analytical LM4 solution, actuator case. LD2 and LM2 FEs are employed for PVD and RMVT case, respectively. The electric displacement is in $[c/m^2]$. $D_z = D_z(a/2, b/2)$. The D_z RMVT-$D_z{}^*$ is calculated by constitutive relations in the RMVT-D_z analysis.

R_β/h	2	4	10	100
		Φ a $z=0$		
LD4	0.3431	0.4611	0.5037	0.5254
LM1	0.5000	0.5000	0.5000	0.5000
LM2	0.3415	0.4609	0.5037	0.5254
LM3	0.3436	0.4614	0.5037	0.5254
LM4	0.3431	0.4611	0.5037	0.5254
		$\mathcal{D}_z 10^{11}$ a $z=h/2$		
LD4	−605.73	−801.76	−1622.9	−10416
LM1	−327.37	−642.20	−1599.7	−16656
LM2	−529.21	−743.93	−1593.3	−16262
LM3	−587.25	−787.72	−1616.7	−16266
LM4	−584.80	−783.99	−1615.6	−16266

Table 8. Proposed benchmark: one piezoelectric layer for the Varadan and Bhaskar cylindrical shell. Comparison of various approaches. Actuator case.

R_β/h	2	4	10	100
		Φ a $z=0$		
LD4	0.0153	0.0355	0.0942	0.6513
LM1	0.0000	0.0000	0.0000	0.0000
LM2	0.0150	0.0350	0.0939	0.6513
LM3	0.0161	0.0359	0.0943	0.6514
LM4	0.0153	0.0355	0.0942	0.6513
		$\mathcal{D}_z 10^{9}$ a $z=h/2$		
LD4	0.0224	0.1377	2.0958	1456.1
LM1	−0.1340	−0.3506	−1.7252	−197.53
LM2	0.0407	0.0378	−0.0937	−111.27
LM3	0.0045	0.0092	−0.1536	−111.76
LM4	0.0095	0.0028	−0.1646	−111.76

Table 9. Proposed benchmark: one piezoelectric layer for the Varadan and Bhaskar cylindrical shell. Comparison of various approaches. Sensor case.

R_β/h	2	4	10	100
		Φ a $z = 0$		
LD4	0.4064	0.4829	0.5029	0.5009
LM1	0.3805	0.4784	0.5041	0.5012
LM2	0.4059	0.4827	0.5029	0.5009
LM3	0.4065	0.4829	0.5029	0.5009
LM4	0.4064	0.4829	0.5029	0.5009
		$\mathcal{D}_z 10^9$ a $z = h/2$		
LD4	−1.0754	−0.6666	−0.3322	−0.3494
LM1	−1.0844	−0.6674	−0.3285	−0.3623
LM2	−1.0639	−0.6600	−0.3268	−0.3622
LM3	−1.0655	−0.6603	−0.3269	−0.3622
LM4	−1.0654	−0.6603	−0.3269	−0.3622

Table 10. Proposed benchmark: multilayered piezoelectric Varadan and Bhaskar cylindrical shell. Comparison of various approaches. Actuator case.

R_β/h	2	4	10	100
		Φ a $z = 0$		
LD4	0.0039	0.0157	0.0485	0.3414
LM1	0.0013	0.0133	0.0458	0.3287
LM2	0.0038	0.0156	0.0485	0.3414
LM3	0.0039	0.0157	0.0485	0.3414
LM4	0.0039	0.0156	0.0485	0.3414
		$\mathcal{D}_z 10^{11}$ a $z = h/2$		
LD4	9.8912	42.445	391.73	227910
LM1	1.1188	1.6464	1.9872	−1.6061
LM2	0.5401	0.6890	0.8068	−2.5408
LM3	0.6220	0.7813	0.9010	−2.4677
LM4	0.6092	0.7747	0.9001	−2.4676

Table 11. Proposed benchmark: multilayered piezoelectric Varadan and Bhaskar cylindrical shell. Comparison of various approaches. Sensor case.

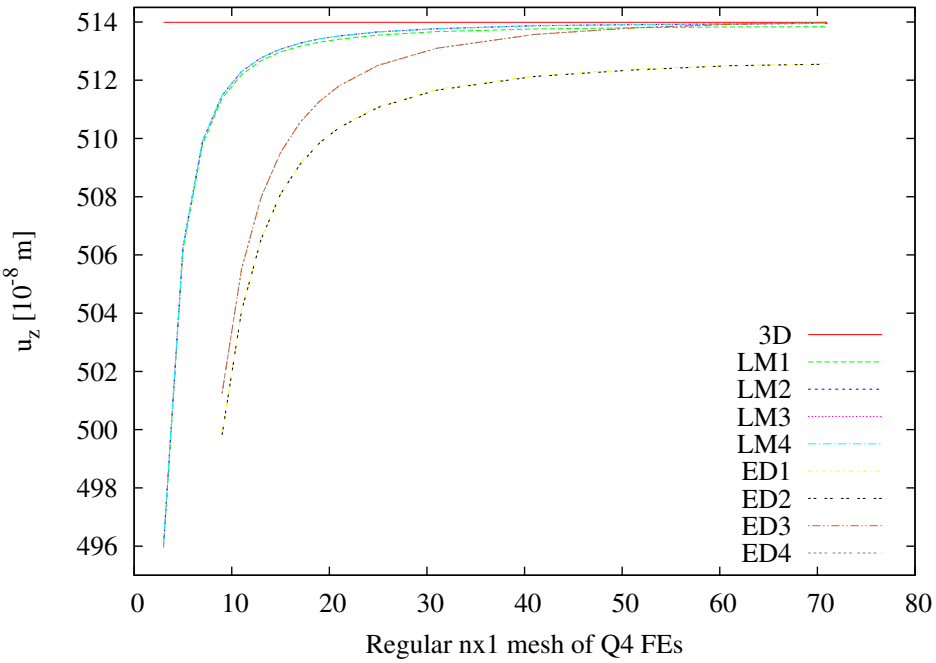

Figure 1. Midplane transverse displacement at the center of the plate: convergence study

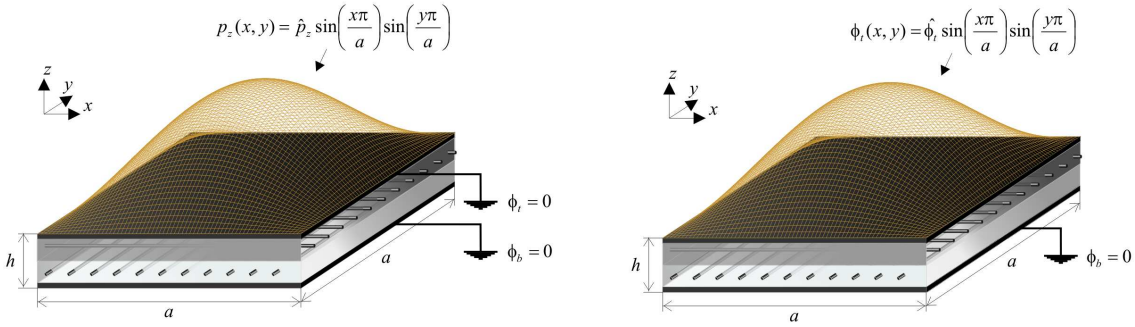

Figure 2. On the left the plate in sensor configuration (applied pressure); on the right the plate in actuator configuration (applied potential)

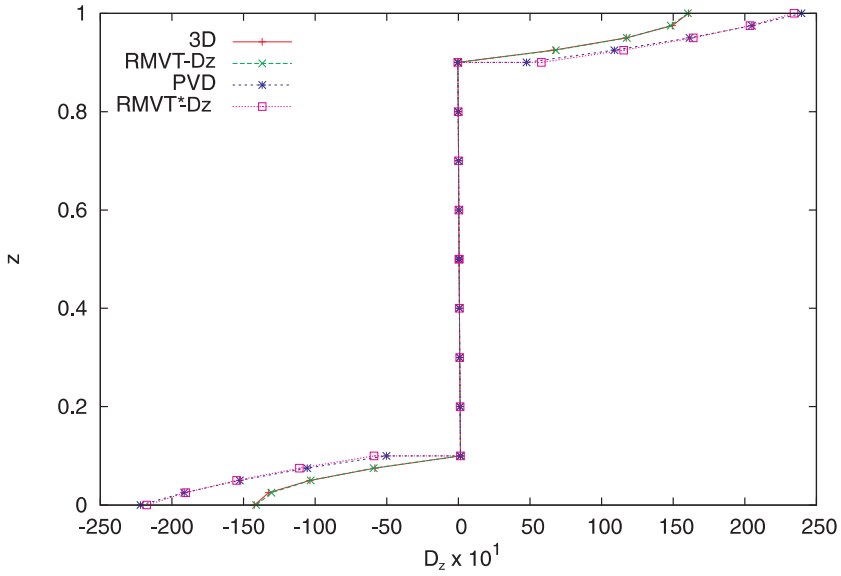

Figure 3. Comparison between FEM and 3D-exact solutions, sensor case; the electric displacement is in $[c/m^2]$; $D_3 = D_3(a/2, b/2)$; the D_z RMVT-D_z* is calculated by constitutive relations in the RMVT-D_z analysis

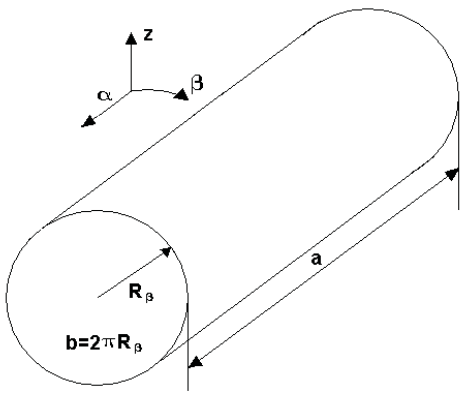

Figure 4. Proposed benchmark: Varadan and Bhaskar cylindrical shell, geometry and notation